Ocean Engineering 52 (2012) 75–82

Contents lists available at SciVerse ScienceDirect

Ocean Engineering

journal homepage: www.elsevier.com/locate/oceaneng

Evaluation of vertical and horizontal bearing capacities of bucket foundations in clay

Le Chi Hung, Sung Ryul Kim *

Civil Engineering Department, Dong-A University, 840 Hadan2-dong, Saha-gu, Busan 604-714, Korea

ARTICLE INFO

Article history:
Received 2 January 2012
Accepted 2 June 2012
Editor-in-Chief: A.I. Incecik
Available online 28 June 2012

Keywords:
Bucket foundation
Clay
Bearing capacity
Finite element analyses
Undrained shear strength

ABSTRACT

The present paper presents the results of three-dimensional finite element analyses of bucket foundations in normally consolidated uniform clay under undrained conditions. The stress–strain response of clay was simulated using the Tresca criterion. The bearing capacities were calculated and found to be largely dependent on the aspect ratio of the bucket foundation. Based on the results of the analyses, new equations were proposed for calculating vertical and horizontal bearing capacities. In the proposed equations, the vertical capacity consisted of an end-bearing resistance and a skin friction resistance, whereas the horizontal capacity consisted of a normal resistance, a radial shear resistance, and a base shear resistance. Comparison of the numerical results showed that the proposed equations properly predicted the capacities of the bucket foundations in uniform or non-uniform clays.

1. Introduction

A bucket foundation is a circular surface foundation with thin skirts around the circumference. Bucket foundations have been used extensively in offshore facilities, such as platforms, wind turbines, or jacket structures (Tjelta and Haaland, 1993; Bransby and Randolph, 1998; Houlsby et al., 2005; Luke et al., 2005).

The skirt of a bucket foundation is first penetrated into the seabed by a self-weight. Further penetration is achieved by pumping water out of the bucket foundation, creating a suction pressure inside it. Penetration stops when the top-plate of the bucket comes in contact with the seabed, and the suction pressure confines a plugged soil within the skirt.

Several studies on bucket foundations in clay have been conducted. Previous numerical studies assumed that the foundation was either a skirted strip foundation in two-dimensional (2D) finite element (FE) analyses (Bransby and Randolph, 1998, 1999; Yun and Bransby, 2007a,b; Gourvenec, 2008; Bransby and Yun, 2009) or an equivalent surface circular foundation in three-dimensional (3D) FE analyses without modeling the embedment of the foundation (Tani and Craig, 1995; Bransby and Randolph, 1998). A few numerical studies have performed 3D FE analyses on bucket foundations for wind turbines (Zhan and Liu, 2010), and suction anchor cases (Sukumaran et al., 1999; Monajemi and Razak, 2009). The bearing capacity of the bucket foundation is significantly affected by the skirt embedment depth or 3D shape. Deeper embedment of the bucket foundation induces more vertical and horizontal capacities attributable to the mobilization of the side friction and the lateral resistance along the skirt. A 3D geometry of the foundation should be modeled to consider the shape effect and the soil–bucket interaction.

In addition, previous design equations have been developed based on numerical results, which have the aforementioned limitations. Therefore, the development of design equations based on accurate numerical results, which consider 3D soil-structure interactions and the exact shape of the bucket foundation is necessary.

In the present study, a series of 3D FE analyses were performed to evaluate the effect of the aspect ratios of the bucket foundation, L/D, where L is the skirt length and D is foundation diameter, on the vertical (V_0) and horizontal (H_0) bearing capacities of bucket foundations for wind turbines. The L/D ratio is usually less than 1.0, as shown in Fig. 1. The soil condition was assumed to be normally consolidated uniform clay. The vertical and the horizontal loadings were applied, and the effect of the L/D ratio on the capacity was carefully analyzed. Simple design equations were developed based on the results of the analyses to evaluate vertical and horizontal capacities.

2. Numerical modeling

For a short-term stability problem of saturated clays, the undrained condition can reasonably be assumed to carry out total stress analyses (Tani and Craig, 1995). Therefore, the soil in the present study was modeled as a linear elastic-perfectly plastic

* Corresponding author. Tel.: +82 51 200 7622; fax: +82 51 201 1419.
E-mail address: sungryul@dau.ac.kr (S.R. Kim).

0029-8018/$ - see front matter © 2012 Elsevier Ltd. All rights reserved.
http://dx.doi.org/10.1016/j.oceaneng.2012.06.001

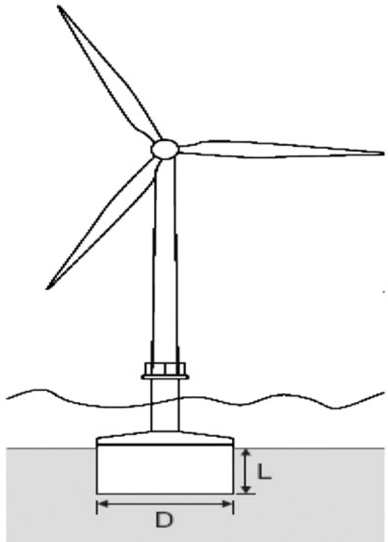

Fig. 1. Bucket foundation for wind turbines (after Houlsby et al., 2005).

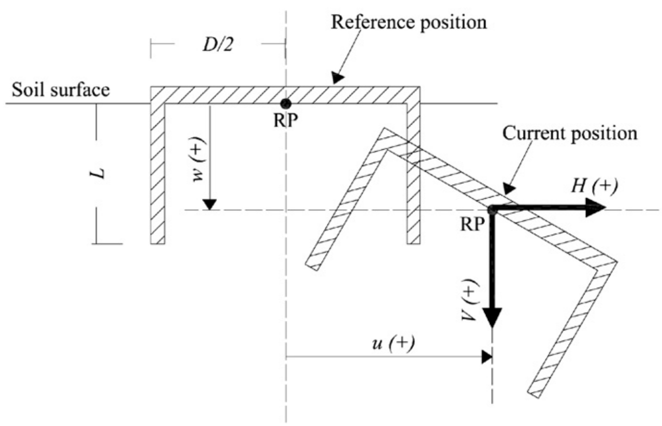

Fig. 2. Bucket foundation geometry and sign convention for loads and displacements (modified after Villalobos et al., 2010).

model based on the Tresca failure criterion ($\phi=0^{\circ}$ condition). The uniform undrained shear strength of the clay (S_u) was assumed to be 5 kPa with a Young's modulus (E_u) at $400\times S_u$. A Poisson's ratio of $v=0.495$ was applied to simulate the constant volume response of clay under undrained conditions (Yun and Bransby, 2007b; Taiebat and Carter, 2000). The effective unit weight of soil at $\gamma'=6$ kN/m^3, was applied. The bucket foundation had a Young's modulus of $E=E_u\times 10^9$ and was thus considered rigid. The interface between the foundation and the soil was assumed to be rough, and the detachment between the bucket foundation and the soil was prevented (Bransby and Yun, 2009).

All FE analyses were conducted using the ABAQUS software (Simulia, 2010). The first-order, eight-node linear brick, reduced integration continuum with hybrid formulation element C3D8RH was used to model the soil.

Fig. 2 shows the definition of the bucket foundation geometry and the sign convention adopted in the present study. Loading was applied using the displacement-controlled method, which increases vertical (w) and horizontal (u) displacements at a reference point (RP). In addition, this method is more suitable than the stress-controlled method in obtaining failure load (Bransby and Randolph, 1997; Gourvenec and Randolph, 2003).

Fig. 3 exhibits a typical mesh used in the present study. Displacements at the bottom boundary were fully fixed for the x, y, and z

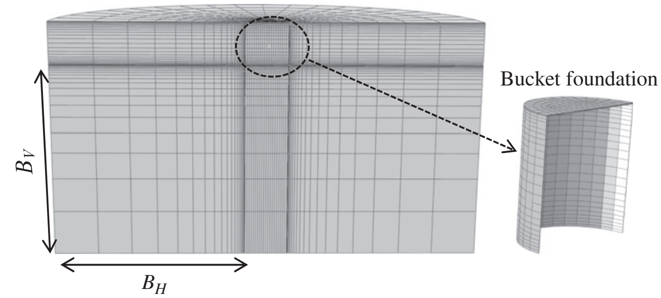

Fig. 3. Definition of boundary extensions and a typical mesh for bucket foundations.

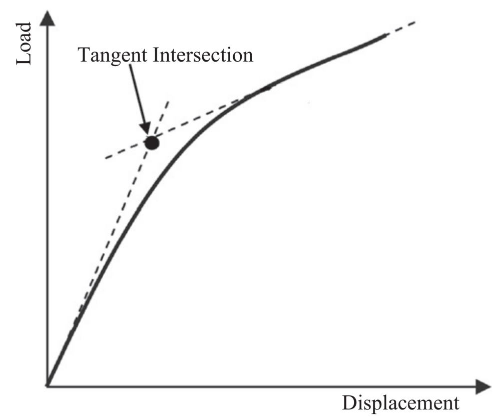

Fig. 4. Tangent intersection method for determining bearing capacity (modified after Mosallanezhad et al., 2008).

directions. Normal displacements at the lateral boundaries were constrained. By applying symmetric conditions, half of the entire system was modeled. The size of the soil elements increased gradually from the bucket foundation to the domain boundary. B_V and B_H are the vertical and horizontal boundary extents from the skirt tip and the side of the bucket foundation, respectively. The bearing capacities gradually decreased as B_H/D or B_V/D increased and became constant at $B_H/D=4.5$ and $B_V/D=4.5$, which were applied for subsequent analyses.

The bearing behavior of the bucket foundation was investigated in terms of normalized bearing capacities $V_0/(A\cdot S_u)$ and $H_0/(A\cdot S_u)$, where V_0 and H_0 are the vertical and horizontal bearing capacities respectively, and A is the cross-sectional area of the bucket. The bearing capacities V_0 and H_0 were determined using the tangent intersection method (Mansur and Kaufman, 1956), as shown in Fig. 4. The method plots two tangential lines along the initial and later portions of the load-displacement curve, and the load corresponding to the intersection point of these two lines is taken as the bearing capacity.

The aspect ratio of the bucket foundation (L/D ratio) varied at 0.1, 0.2, 0.25, 0.3, 0.5, 0.6, 0.75, 0.85, and 1.0. The skirt thickness $t_{skirt}=0.004D$ and top plate thickness $t_{plate}=0.01D$ were applied. Preliminary analyses confirmed that the bucket foundation diameter D had no effect on the normalized bearing capacities. Hence, D was kept at 10 m.

3. Analysis results

3.1. Vertical bearing behavior of the bucket foundations

Fig. 5 presents the normalized vertical load-displacement curves and the vertical capacity of the bucket foundations

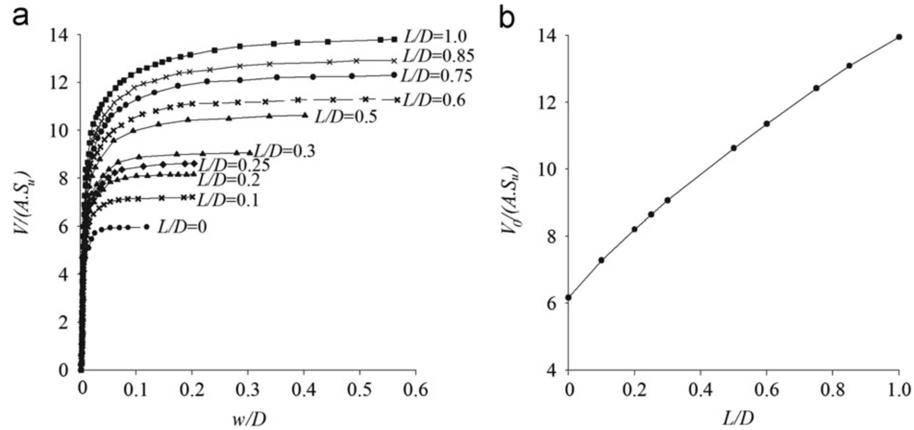

Fig. 5. Vertical load-movement curve and capacity according to L/D ratios.

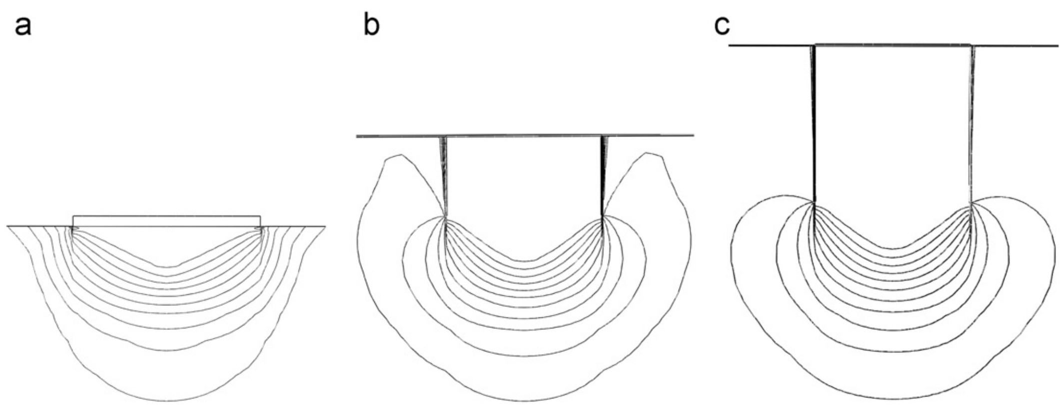

Fig. 6. Failure mechanism under vertical load according to L/D ratios. (a) $L/D=0$, (b) $L/D=0.5$ and (c) $L/D=1.0$.

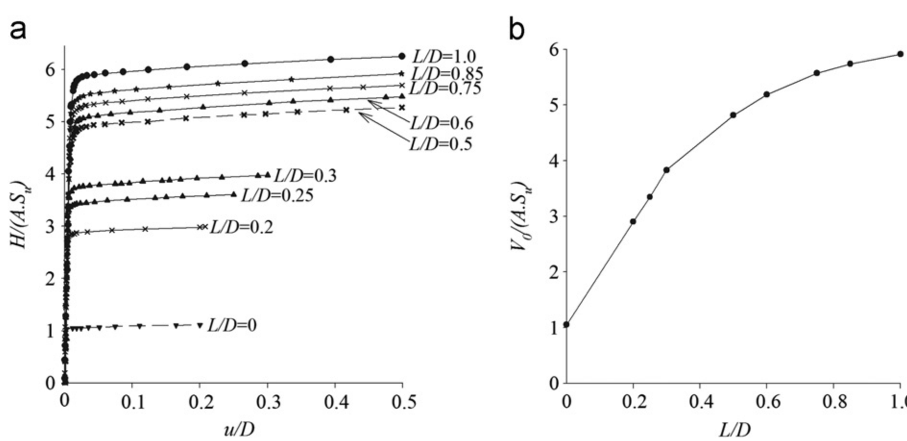

Fig. 7. Horizontal load-movement curve and capacity according to L/D ratios.

according to the L/D ratios. At the surface foundation ($L/D=0$), $V_0/(A \cdot S_u)=5.95$ was obtained, which was only an underestimation of 1.6% compared with the exact value of 6.05 (Eason and Shield, 1960; Houlsby and Worth, 1983).

The vertical bearing capacity increased with increasing L/D ratio. The increasing rate of the vertical capacity with the L/D ratio slightly decreased at $L/D=0.5$, and then became almost constant after $L/D=0.5$. The non-linear increase in the vertical capacity can be explained by the transition of the failure mechanism, as illustrated in Fig. 6, from a traditional Prandtl surface failure (Fig. 6(a)) to a flow mechanism (Fig. 6(b)) and then to a confined mechanism (Fig. 6(c)). The phenomenon is similar to that reported by Mana et al. (2011).

3.2. Horizontal bearing behavior of bucket foundations

Fig. 7 shows the normalized horizontal load-displacement curves and the horizontal capacity of the bucket foundations according to the L/D ratios. The horizontal bearing capacity

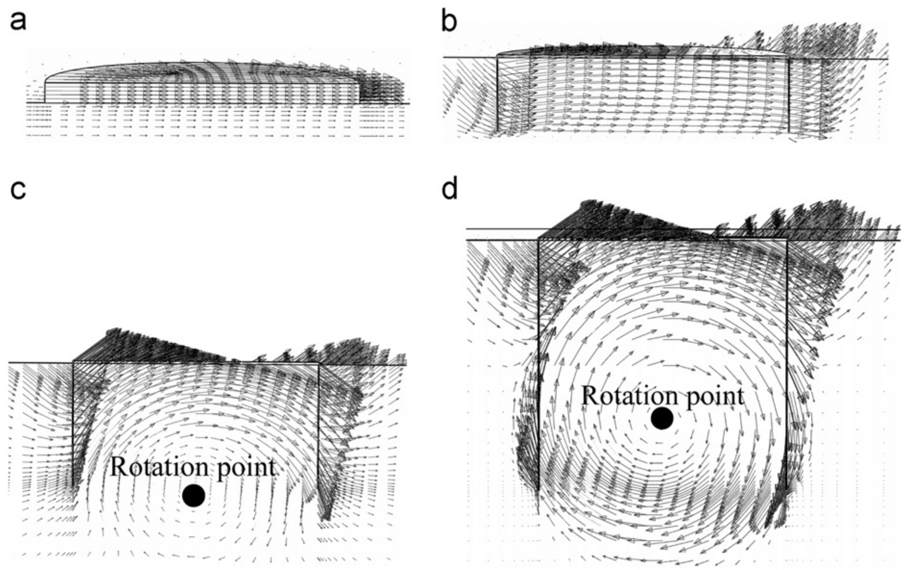

Fig. 8. Failure mechanisms under horizontal load according to L/D ratios. (a) $L/D=0$, (b) $L/D=0.25$, (c) $L/D=0.5$ and (d) $L/D=1.0$.

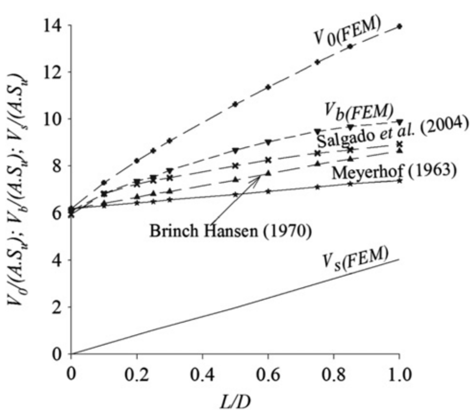

Fig. 9. Comparison of vertical bearing capacities.

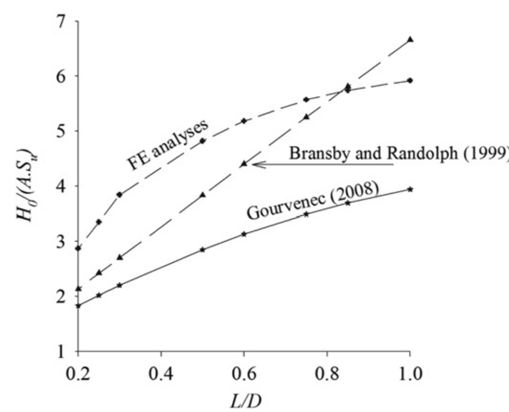

Fig. 10. Comparison of horizontal bearing capacities.

increased linearly at $L/D<0.5$, and the increasing rate decreased at $L/D \geq 0.5$.

The decrease in the increasing rate can be explained by the change in the failure mechanism under the horizontal load. A pure sliding behavior was occurred at $L/D=0$, whereas a sliding behavior with minimal rotation was observed at $L/D=0.25$, as shown in Fig. 8(a) and (b). At $L/D \geq 0.5$, the rotational behavior became significant, as shown in Fig. 8(c) and (d). Hence, the failure mode of the bucket foundation under the horizontal load changed from a purely horizontal translation to a combination of horizontal and rotational translations with increasing L/D ratios (Gourvenec, 2008).

3.3. Comparison with previous methods

The bucket foundation can be considered as an embedded shallow foundation. Thus, the present design codes applied the conventional design methods of shallow foundations by adopting several factors, such as foundation shape, load inclination, and embedment depth. For the bucket foundation in undrained clay, the vertical bearing capacity can be expressed by Eq. (1). In the present study, the vertical load was presumably applied at the center of the foundation. Thus, the eccentric factor was $d_e=1$, and the load inclination factor was $d_i=1$.

$$V_0 = N_c d_s d_{cV} d_e d_i A S_u \tag{1}$$

where, N_c is the bearing capacity factor and $N_c=5.14$ is for a strip foundation (Houlsby and Worth 1983); d_s is the shape factor and $d_s=1.2$ is for a circular surface rough foundation (Skemton, 1951; Meyerhof, 1963; Brinch Hansen, 1970); d_{cV} is the depth factor, and $d_{cV}=1+n(L/D)$, where $0.2 \leq n \leq 0.4$ (Skemton, 1951; Meyerhof, 1963; Brinch Hansen, 1970); d_e is the load eccentricity factor; and d_i is the load inclination factor

The results of the FE analyses were compared with those of previous methods. The capacities predicted by conventional methods using Eq. (1) are indicated as "Salgado et al (2004)" "Meyerhof (1963)" and "Brinch Hansen (1970)", as shown in Fig. 9. A comparison with the FE analyses results, indicated as "$V_{0(FEM)}$," showed that the conventional methods underestimated the capacity, and that the difference between the prediction and the FE analyses results increased with the L/D ratios. The primary reason for the underestimation is the fact that conventional methods do not consider skin friction along the skirt of the bucket.

Fig. 10 shows a comparison of the horizontal capacity for different bucket foundations from the FE analyses and other published solutions. The solution by Gourvenec (2008) and the upper bound solution by Bransby and Randolph (1999) underestimated the capacity, except for $L/D=1.0$ using the solution by Bransby and Randolph (1999). This phenomenon can be explained by the effect of the foundation shape because the solutions by Gourvenec (2008) and Bransby and Randolph (1999) consider the foundations in 2D. By contrast, the present study performed solution in 3D. In addition, the bearing capacities from the Bransby and Randolph (1999) solution showed a linear increase with increasing L/D ratios. The primary reason for this is that the Bransby and Randolph (1999) solution does not consider the combination of horizontal and rotational translations with increasing L/D ratios.

4. Development of bearing capacity equations

Simple design equations were proposed for evaluating the vertical and horizontal bearing capacities of the bucket foundation. The equations divided the bearing capacity into several components, which were evaluated based on the results of the numerical analyses.

4.1. Vertical capacity

The published solutions underestimated the vertical capacity of the bucket foundations. Therefore, several studies (House and Randolph, 2001; Byrne and Cassidy, 2002; Yun and Bransby, 2007b; Zhan and Liu, 2010) suggested that the vertical bearing capacity can be determined by summing up two components, namely, end-bearing resistance (V_b) and skin friction resistance (V_s), as shown in Fig. 11.

$$V_0 = V_b + V_s \tag{2}$$

V_b can be evaluated using Eq. (3), which has the same form of the conventional methods as Eq. (1).

$$V_b = N_c d_s d_{cV} A S_u \tag{3}$$

A comparison between the $V_{b(FEM)}$ curve and the curves of previous methods is shown in Fig. 9. As shown in the figure, the d_{cV} factors in the conventional methods do not properly predict the L/D ratio effect on the capacity. Therefore, the depth factor d_{cV} was back-calculated by adopting $V_{b(FEM)}$ from the FE analyses using Eq. (3), where N_c=5.14, and d_s=1.2. $V_{b(FEM)}$ was evaluated by averaging the vertical stresses in soil elements immediately below the skirt tip level following the method of Yun and Bransby (2007b).

Fig. 12 shows the back-calculated d_{cV} according to the L/D ratios, and Eq. (4) was suggested to evaluate V_b. Interestingly, the form of Eq. (4) is similar to that obtained by Gourvenec (2008) for strip foundations.

$$d_{cV} = 1 + 1.02\left(\frac{L}{D}\right) - 0.42\left(\frac{L}{D}\right)^2 \tag{4}$$

The $V_{s(FEM)}$ curve shown in Fig. 9 was obtained as the average frictional stress components acting on the skirt. The curve revealed

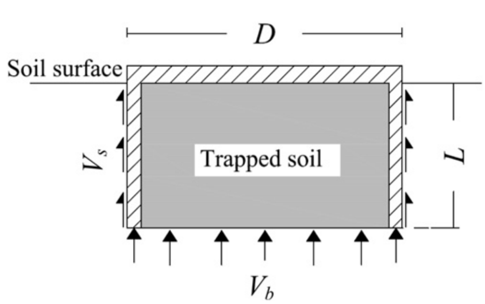

Fig. 11. Definition of end-bearing resistance (V_b) and skin friction resistance (V_s).

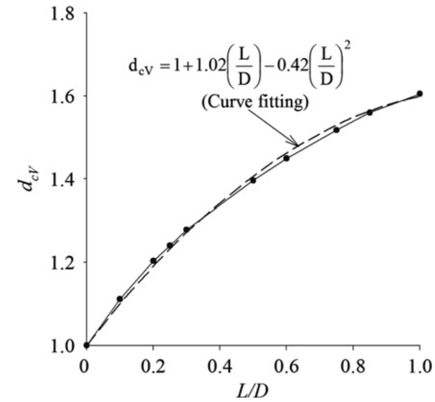

Fig. 12. Depth factor d_{cV} *versus* L/D ratios.

that the normalized $V_{s(FEM)}$ linearly increased with increasing L/D ratios, indicating that V_s was only proportional to the side area and S_u. Therefore, V_s can be calculated by introducing the α factor:

$$V_s = \alpha \pi L D S_u \tag{5}$$

where α is the adhesion factor. For normally consolidated clay with $S_u \leq 50$ kPa, $\alpha=1$ (Das, 1999).

4.2. Horizontal capacity

The horizontal capacity of the bucket foundations can be predicted by analyzing the stress distribution along the bucket under the horizontal load. Fig. 13(a) presents the active (σ_{a1}, σ_{a2}) and passive (σ_{p1}, σ_{p2}) stresses, as well as the radial (τ_{r1}, τ_{r2}) and the base (τ_b) shear stresses mobilized on the foundation under the horizontal load, as suggested by Reese and Sullivan (1980) and Bang and Cho (2001).

Notably, the numerical results exhibited that the failure mechanism of the bucket foundation under the horizontal load changed according to the L/D ratios. Therefore, stress distribution along the bucket foundation was classified into two cases. One was the stress acting on the bucket foundation with the combination of rotational and horizontal translations for $L/D \geq 0.5$, as shown in Fig. 13(a). The other was the stress acting on the bucket foundation with a purely horizontal translation for $L/D < 0.5$, as shown in Fig. 13(b).

The horizontal bearing capacity can be calculated using Eqs. (6) and (7) based on the force equilibrium along the loading direction.

$$H_0 = P_u + T_{side} - T_{base} \quad L/D \geq 0.5 \tag{6}$$

$$H_0 = P_u + T_{side} + T_{base} \quad L/D < 0.5 \tag{7}$$

where P_u is the normal resistance, T_{side} is the radial shear resistance, and T_{base} is the base shear resistance.

Each component in the horizontal capacity was evaluated as follows:

4.2.1. Normal resistance (P_u)

According to the equilibrium condition in Fig. 13, the normal pressure (p_u) along the loading direction for the bucket foundation can be expressed as Eqs. (8) and (9).

$$p_u = \sigma_{p1} + \sigma_{a2} - \sigma_{a2} - \sigma_{p2} \quad L/D \geq 0.5 \tag{8}$$

$$p_u = \sigma_{p1} - \sigma_{a1} \quad L/D < 0.5 \tag{9}$$

Fig. 13(c) shows the distributions of p_u and τ_r along the bucket foundation circumference. The normal stress p_u becomes the maximum and minimum values at $\theta=0$ and $\theta=\pm\pi/2$, respectively. The radial shear stress reaches the maximum and minimum values at $\theta=\pm\pi/2$ and $\theta=0$, respectively.

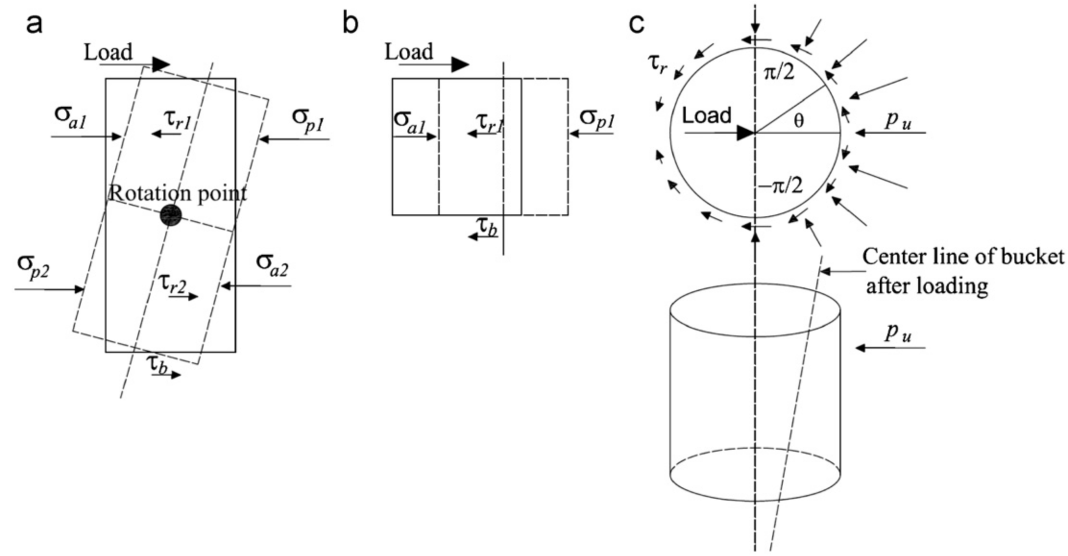

Fig. 13. Distribution of stresses along bucket foundation under horizontal load (modified after Reese and Sullivan, 1980; Bang and Cho, 2001). (a) $L/D \geq 0.5$, (b) $L/D < 0.5$ and (c) Plan view

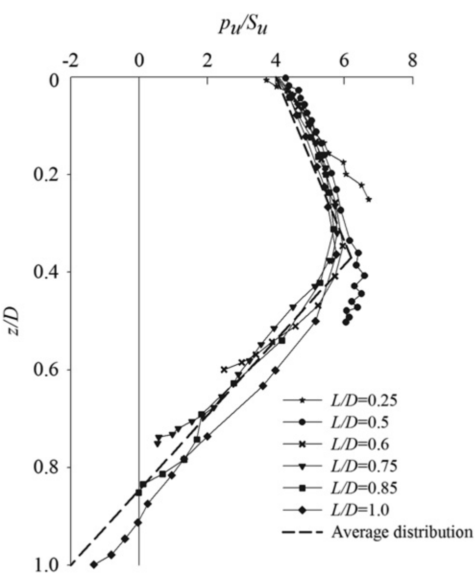

Fig. 14. Normal horizontal stress distributions along bucket foundation.

The active and passive stresses developed on the bucket foundation were calculated by averaging lateral stress components in the outer soil elements immediately adjacent to the skirt.

Fig. 14 presents the variations of a normalized p_u/S_u and a normalized depth z/D (where z is the depth below the ground surface) for different L/D ratios. The results showed that p_u was approximately $4S_u$ at the ground surface for all cases, which then increased linearly up to a depth of $z=0.37D$. Below $z=0.37D$, p_u/S_u decreased linearly and had the opposite direction below a depth of $z=0.9D$. Interestingly, the distribution shape of the normal resistance in this study was similar to that obtained by Prasad and Chari (1999) for a short pile in cohesionless soil.

The following two equations were proposed to fit the average values of p_u/S_u:

$$p_u = \left(4+5.95\frac{z}{D}\right) \times S_u \quad 0 \leq z/D \leq 0.37 \tag{10}$$

$$p_u = \left(11.02-13.02\frac{z}{D}\right) \times S_u \quad z/D > 0.37 \tag{11}$$

The normal resistance, P_u can then be calculated by integrating p_u along depth as follows:

$$P_u = 0.5\int_0^L p_u \pi D dz \tag{12}$$

4.2.2. Radial shear resistance (T_{side})

Radial shear stresses (τ_r) on the bucket foundation were obtained by averaging the radial shear stress components in the outer soil elements immediately adjacent to the skirt.

Fig. 15 presents a normalized τ_r/S_u with z/D. τ_r/S_u was approximately -0.26 from the ground surface to a depth of $z=0.5D$ for all cases. τ_r/S_u increased linearly to an approximately positive value of $\tau_r/S_u=0.26$. In addition, τ_r/S_u became zero at different depths with different L/D ratios.

The average values of τ_r/S_u were fitted by Eq. (13), which applied upper and lower limit values of 0.26 and -0.26, respectively.

$$-0.26 \leq \frac{\tau_r}{S_u} = \left[5.2\frac{z}{D}-\left(2.5\frac{L}{D}+1.4\right)\right] \leq 0.26 \tag{13}$$

Radial shear resistance can be calculated by integrating τ_r along the depth as follows:

$$T_{side} = \int_0^L \tau_r \pi D dz \tag{14}$$

4.2.3. Base shear resistance (T_{base})

The base shear stress, τ_b, at the skirt tip level of the foundation can be calculated as $\alpha \times S_u$ in Eq. (5). Therefore, the base shear resistance can be given by

$$T_{base} = \tau_b \times A \tag{15}$$

5. Discussions

The undrained shear strength of clay varies with depth and the non-uniformity of clay should be considered for practical design. Therefore, additional analyses on the non-uniform clay were performed. The undrained shear strength of the clay was assumed to linearly increase with depth and had a general form of $S_u=S_{um}+kz$, as shown in Fig. 16. The kD/S_{um} value, which defines the increasing ratio of the undrained shear strength with depth, varied at 0.2, 0.4, 0.6 and ∞ in the additional analyses.

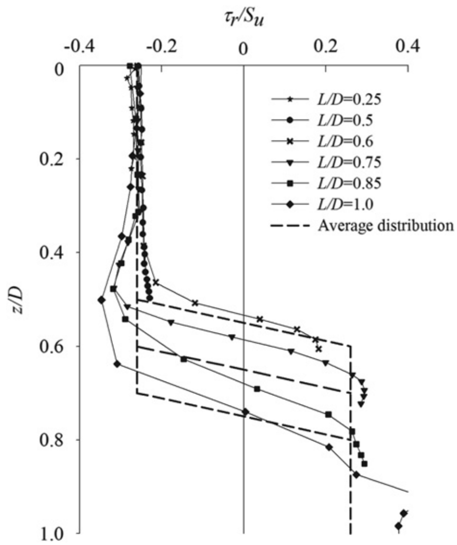

Fig. 15. Radial shear stress distributions along bucket foundation.

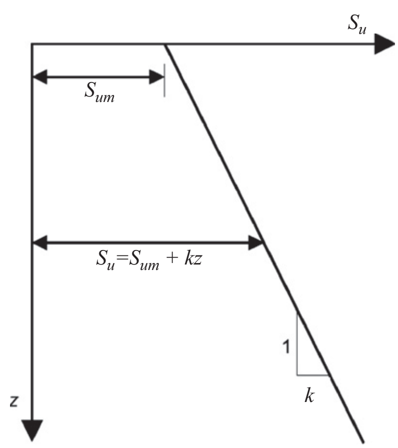

Fig. 16. Variation of undrained shear strength with depth (S_{um}=the undrained shear strength of clay at ground surface; k is the strength gradient; z is the depth below ground surface).

In the proposed equations, the undrained shear strength at different depths was adopted to consider the non-uniformity of the clay.

Vertical capacity consisted of the end-bearing resistance V_b and the skin friction resistance V_s. To evaluate V_b, several researchers suggested that S_u can be selected as the value at depth $D/3$ (Skemton, 1951) or $D/4$ (Byrne and Cassidy, 2002) below the skirt tip. In the present study, S_u in Eq. (3) was selected as the value at depth $D/10$ below the skirt tip to match the FE results. The S_u for evaluating V_s in Eq. (5) can be selected as an average S_u along the skirt length L. This procedure was also suggested by Yun and Bransby (2007b).

Horizontal capacity consisted of the normal resistance P_u, the radial shear resistance T_{side} and the base shear resistance T_{base}. S_u for evaluating P_u and T_{side} in Eqs. (10), (11) and (13) was selected as the S_u value at depth $2L/3$ from the ground surface. T_{base} can be evaluated using S_u at the depth of skirt tip level.

Tables 1 and 2 compare the predicted capacities from the proposed equations with those from the FE analyses. The predicted capacities in the uniform clay ($kD/S_{um}=0$) condition was also compared in the tables. The differences between the proposed equations and the FE analyses for the vertical and horizontal capacities were only 0%–5.96% and 0%–10.23%, respectively. Therefore, the proposed equations can be ideally applied for the prediction of the capacity of the buckets in uniform and non-uniform clays under undrained conditions.

Table 1
Comparison of normalized vertical bearing capacity $V_0/(A \cdot S_{u(base)})$.

	$L/D=0.25$		$L/D=0.5$		$L/D=0.75$		$L/D=1.0$	
	Proposed	FEM	Proposed	FEM	Proposed	FEM	Proposed	FEM
kD/S_{um}								
0	8.58	8.75	10.67	10.78	12.43	12.47	13.87	13.95
2	9.39	9.96	10.93	11.12	12.10	12.05	12.93	12.88
4	9.79	10.41	11.02	11.13	12.02	11.61	12.74	12.45
6	9.96	10.55	10.88	10.86	11.69	11.45	12.24	12.27
∞	10.86	11.51	10.90	10.81	11.44	11.44	11.86	11.93
Error (%)	2.00–5.96		0.18–1.71		0.00–3.53		0.24–2.33	

Note: $S_{u(base)}$=undrained shear strength of clay at the skirt tip level.

Table 2
Comparison of normalized horizontal bearing capacity $H_0/(A \cdot S_{u(base)})$.

	$L/D=0.25$		$L/D=0.5$		$L/D=0.75$		$L/D=1.0$	
	Proposed	FEM	Proposed	FEM	Proposed	FEM	Proposed	FEM
kD/S_{um}								
0	3.65	3.35	4.43	4.82	6.14	5.57	5.92	5.92
2	3.19	3.08	3.73	4.00	4.68	4.34	4.15	4.19
4	3.09	2.95	3.41	3.67	4.33	4.01	3.86	3.86
6	3.00	2.85	3.25	3.50	4.16	3.85	3.73	3.72
∞	2.72	2.58	2.78	3.02	3.73	3.46	3.41	3.34
Error (%)	3.57–8.96		6.75–8.09		7.80–10.23		0.00–2.10	

6. Conclusion

This paper presents the results of three-dimensional numerical analyses of the bucket foundations in normally consolidated clay. The following conclusions were drawn from the present study.

1) The vertical bearing capacity of the bucket foundation was properly evaluated via FE analyses. The vertical bearing capacity increased with increasing L/D ratios. However, the increase in the vertical bearing capacity was not linear because of the transition of the failure mechanism, from a traditional Prandtl surface failure to a flow mechanism and subsequently, to a confined mechanism.
2) The horizontal bearing capacity increased with increasing L/D ratio. A linear increase of the horizontal bearing capacity was observed for foundations with $L/D<0.5$, whereas a non-linear increase was observed for those with $L/D \geq 0.5$. These phenomena can be attributed to the effects of the combination between horizontal and rotational translations from the increase in L/D ratios. Hence, the effects of this combination became more significant as more rotation and less sliding governed the failure.
3) Simple equations were proposed for calculating the vertical and horizontal bearing capacities of the bucket foundations in undrained clay. The vertical bearing capacity of the bucket foundations can be obtained via two components, namely, the end-bearing resistance and the skin friction resistance. The horizontal capacity in the proposed equations consisted of the normal resistance, radial shear resistance, and base shear resistance. Comparison between the results of the FE analyses and the proposed equations showed that the proposed equations can be used to evaluate the vertical and horizontal

capacities of the bucket foundations in uniform and non-uniform clays under undrained conditions.

Acknowledgments

The present research was supported by the 2010 Construction Technology Innovation Program funded by the Korea Institute of Construction and Transportation Technology Evaluation and Planning (KICTTEP) and the Ministry of Land, Transport, and Maritime Affairs (MLTM) (No.10-CTIP-E04), and by the Basic Science Research Program through the National Research Foundation of Korea (NRF) funded by the Ministry of Education, Science and Technology (No.2010-0022382).

References

Bang, S.C., Cho, Y.K., 2001. Ultimate horizontal loading capacity of suction piles. In: Proceedings of the 11th International Offshore and Polar Engineering Conference, Stavanger, Norway, 552–559.

Brinch Hansen, J., 1970. A Revised and Extended Formula for Bearing Capacity. Bulletin No. 28. Danish Geotechnical Institute.

Byrne, B.W., Cassidy, M.J., 2002. Investigating the response of offshore foundations in soft clay soils. In: Proceedings of the 21st International Conference on Offshore Mechanics and Arctic Engineering OMAE'02, Oslo, paper OMAE2002-28057.

Bransby, M.F., Randolph, M.F., 1997. Shallow foundations subject to combined loadings. In: Proceedings of the 9th International Conference on Computer Methods and Advances in Geomechanics, Wuhan 3, 1947–1956.

Bransby, M.F., Randolph, M.F., 1998. Combined loading of skirted foundations. Géotechnique 48 (5), 637–655.

Bransby, M.F., Randolph, M.F., 1999. The effect of embedment depth on the undrained response of skirted foundations to combined loading. Soils Found. 39 (4), 19–33.

Bransby, M.F., Yun, G., 2009. The undrained capacity of skirted strip foundation under combined loading. Géotechnique 59 (2), 115–125.

Das, B.M., 1999. Principles of Foundations Engineering, 4th edition 152–217.

Eason, G., Shield, R.T., 1960. The plastic indentation of a semi-infinite solid by a perfectly rough circular punch. Z. Angew. Math. Phys. 11, 33–43.

Gourvenec, S., 2008. Effect of embedment on the undrained capacity of shallow foundations under general loading. Géotechnique 58 (3), 177–185.

Gourvenec, S., Randolph, M.F., 2003. Effect of strength non-homogeneity on the shape of failure envelopes for combined loading of strip and circular foundations on clay. Géotechnique 53 (6), 575–586.

Houlsby, G.T., Worth, C.P., 1983. Calculation of stresses on shallow penetrometers and footings. In: Proceedings of the IUTAM/IUGG Symposium on Seabed Mechanics, Newcastle upon Tyne, September, 107–112.

Houlsby, G.T., Ibsen, L.B., Byrne, B.B., 2005. Suction caissions for wind turbines. In: Gourvenec, Cassidy (Eds.), Frontiers in Offshore Geotechnics: ISFOG 2005. Taylors and Francis group, London 2005.

House, A.R., Randolph, M.F., 2001. Installation and pull out capacity of stiffened suction caissons in cohesive sediments. In: Proceedings of the 11th IOSPE, Stavanger, Norway, 574–580.

Luke, A.M., Rauch, A.F., Olson, R.E., Mecham, E.C., 2005. Components of suction caisson capacity measured in axial pullout tests. Ocean Eng. 32, 878–891.

Mana, D.S.K., Gourvenec, S., Randolph, M.F., 2011. A numerical study of the vertical bearing capacity of skirted foundations. In: Gourvenec, White (Eds.), Frontiers in Offshore Geotechnics II. Taylor & Francis group, London, pp. 433–438 2011.

Mansur, C.I., Kaufman, J.M., 1956. Pile tests, low-sill structure, Old River, Louisiana. J. Soil Mech. Found. Div., ASCE 82 (SM5), 1–33.

Meyerhof, G.G., 1963. Some recent researches on bearing capacity of foundations. Can. Geotech. J. 1, 16–26.

Monajemi, H., Razak, H.A., 2009. Finite element modeling of suction anchors under combined loading. Mar. Struct. 22 (4), 660–669.

Mosallanezhad, M., Hataf, N., Ghahramani, A., 2008. Experimental study of bearing capacity of granular soils, reinforced with innovative grid-anchor system. Geotech. Geol. Eng. 26, 299–312.

Prasad, Y.V.S.N., Chari, T.R., 1999. Lateral capacity of model rigid piles in cohesionless soils. Soils Found. 39 (2), 21–29.

Reese, L.C., Sullivan, W.R., 1980. Documentation of computer program COM 624. The University of Texas 297–325.

Salgado, R., Lyamin, A.V., Sloan, S.W., Yu, H.S., 2004. Two- and three-dimensional bearing capacity of foundation in clay. Géotechnique 54 (5), 297–306.

Simulia, 2010. ABAQUS User's Manual. Dassault Systèmes Simulia Corp.

Skemton, A.W., 1951. The bearing capacity of clays. In: Proceedings of the Building and Research Congress 1, London, 189.

Sukumaran, B., McCarron, W.O., Jeanjean, P., Abouseeda, H., 1999. Efficient finite element techniques for limit analysis of suction caissons under lateral loads. Comput. Geotech. 24, 89–107.

Taiebat, H.A., Carter, J.P., 2000. Numerical studies of the bearing capacity of shallow foundations on cohesive soil subjected to combined loading. Géotechnique 50 (4), 409–418.

Tani, K., Craig, W.H., 1995. Bearing capacity of circular foundation on soft clay of strength increasing with depth. Soils Found. 35 (4), 21–35.

Tjelta, T.I., Haaland, G., 1993. Novel foundation concept for a jacket finding its place. Offshore Site Investig. Found. Behav. 28, 717–728.

Villalobos, F.A., Byrne, B.W., Houlsby, G.T., 2010. Model testing of suction caissons in clay subjected to vertical loading. Appl. Ocean Res. 32, 414–424.

Yun, G., Bransby, M.F., 2007a. The horizontal-moment capacity of embedded foundations in undrained soil. Can. Geotech. J. 44 (4), 409–427.

Yun, G., Bransby, M.F., 2007b. The undrained vertical bearing capacity of skirted foundations. Soils Found. 47 (3), 493–506.

Zhan, Y.G., Liu, F.C., 2010. Numerical analysis of bearing capacity of suction bucket foundation for offshore wind turbines. Electron. J. Geotech. Eng. 15, 633–644.